International Journal of Scientific Engineering and Technology Research

ISSN 2319-8885
Vol.05,Issue.08,
April-2016,
Pages:1662-1674

www.ijsetr.com

Adaptive Load Shedding Based on Combined Frequency and Voltage Stability Assessment using Synchrophasor Measurements

A. SYED SAHEB VALI[1], M. APSAR BASHA[2], A. KANNA KRISHNA GOUD[3], Y. RADHAIAH[4]

[1]PG Scholar, Dept of EEE(EPE), SITAMS, Chittoor, Andhrapradesh, India.
[2]Assistant Professor, Dept of EEE, SITAMS, Chittoor, Andhrapradesh, India.
[3]PG Scholar, Dept of EEE(PE), SITAMS, Chittoor, Andhrapradesh, India.
[4]PG Scholar, Dept of EEE (PE&ED), SVCET, Chittoor, Andhrapradesh, India.

Abstract: Under frequency load shedding (UFLS) and under voltage load shedding (UVLS) are attracting more attention, as large disturbances occur more frequently than in the past. Usually, these two schemes work independently from each other, and are not designed in an integrated way to exploit their combined effect on load shedding. Besides, reactive power is seldom considered in the load shedding process. To fill this gap, we propose in this paper a new centralized, adaptive load shedding algorithm, which uses both voltage and frequency information provided by phasor measurement units (PMUs). The main contribution of the new method is the consideration of reactive power together with active power in the load shedding strategy. Therefore, this method addresses the combined voltage and frequency stability issues better than the independent approaches. The new method is tested on the IEEE 39-Bus system, in order to compare it with other methods. Simulation results show that, after large disturbance, this method can bring the system back to a new stable steady state that is better from the point of view of frequency and voltage stability, and load ability.

Keywords: Adaptive Load Shedding Scheme, Phasor Measurement Units (Pmus), Power System Stability, Synchrophasor, Under Frequency Load Shedding, Under Voltage Load Shedding.

I. INTRODUCTION

Mostly as a consequence of the deregulated electricity markets and the growth of electrical energy consumption, power systems are now often operated close to their stability limits. In case of large disturbances, such as generators tripping and faults on transmission lines leading to cascading faults [1], the resulting active and reactive power imbalance can eventually lead to simultaneous large frequency and voltage deviation, as well as instability. Thus, there is a higher risk that the overall system may collapse. Conventionally, load shedding schemes—under frequency load shedding (UFLS) and under voltage load shedding (UVLS), are designed independently and they constitute the last line of defines against frequency and voltage instability. However, the traditional load shedding schemes are not capable of dealing with combined instabilities, as discussed in [2] and [3]. Since the action of UFLS usually only considers the frequency information, it may have unanticipated, adverse consequences on the voltage. A similar issue affects the conventional UVLS which uses only local voltage magnitude information at the individual buses. Another disadvantage of the conventional methods is that they simply follow a preset rule, such as shedding a fixed percentage of loads when frequency is out of the normal range. This type of rule lacks the flexibility to execute load shedding actions fit for the different type of instabilities. Research work about adaptive UFLS was introduced in [4]–[7] in order to improve the conventional load shedding schemes. However, in these approaches, still only the frequency information is used in the load shedding process.

An improvement has been proposed in [8] and [9], where voltage dependent load modelling has been taken into account for the active power imbalance estimation. Also in this case, though, the voltage information is not exploited for the load shedding strategy. Furthermore, some researchers [10]–[13] have proposed combinational load shedding methods based on adaptive UFLS, in which the distribution of load shedding is determined using the voltage magnitude information. All these combinational load shedding methods go in the direction of addressing the voltage stability issue in adaptive UFLS. However, the existing methods for combinational load shedding still exclude controlled reactive power from the direct participation in load shedding. Instead, we believe that the contribution of resources and equipment capable of reactive power support and control is essential for the voltage stability [14], [15]. With the diffusion of wide-area monitoring and control systems (WAMCS) [16]–[19] based on phasor measurement units (PMUs), the power system stability issues can be addressed more effectively. PMUs can provide synchronized measurements, which include the magnitude and phase angle of voltages and currents, frequency and rate of change of frequency [20].

Copyright @ 2016 IJSETR. All rights reserved.

In [25] and [26], power flow tracing is proposed in a load shedding scheme for the faults originating from lines tripping, and they are proven to work effectively. In this work, we consider the case of generators tripping. By means of the power flow tracing, we can accurately determine the corresponding proportional power of each load bus that is supplied by the lost generators or lines. Usually, the buses in the vicinity of tripping elements are the most sensitive to such kind of faults. This fact leads to load bus selection, and eventually to a reduction of the load busses involved in load shedding. In this paper, we propose a new adaptive load shedding method that considers frequency and voltage stability assessment simultaneously. Such adaptive method is organized in three main steps:

- Determination of a trigger for activating the load shedding procedure;
- Estimation of total power imbalance for the whole system;
- Distribution of the total power imbalance to individual load bus.

The proposed adaptive load shedding method should be applied using both frequency and voltage information at each step, especially in the third step which yields the final load shedding action to be implemented. First, a global voltage stability index and the frequency information for the equivalent inertial center are utilized jointly for the trigger determination. In the second step, we apply a low-order system frequency response (SFR) model [4] combined with the voltage dependent load models [9], to obtain the overall active power mismatch and hence the total amount of reactive power to be shed. Finally, we use both the frequency and voltage information in the third step, for simultaneous active and reactive load shedding distribution. In the active load shedding distribution process, the frequency measurements are used together with the active power estimates provided by tracing power flow. While for the reactive power load shedding distribution, it requires the voltage information combined with reactive power estimates obtained also from tracing power flow. In this way, the appropriate amount of active and reactive power to be shed at the selected buses can be determined simultaneously. Furthermore, the conventional methods have been augmented with reactive power, global voltage stability analysis and load bus selection for load shedding. Thus, the new approach can enhance the recovered steady state with respect to frequency stability, voltage stability and loadability, while also ensuring a good transient behavior, for the same total active power curtailment, compared to the existing load shedding methods.

The structure of this paper is organized as follows: the role of synchrophasors in implementing the proposed adaptive load shedding scheme, and the corresponding algorithms for obtaining the information required in load shedding are described in Section II. The conventional adaptive load shedding is presented in Section III, while Section IV introduces the load shedding method newly proposed, in particular the load shedding distribution determination; test system and platform for the assessment of the proposed method are introduced in Section V, and Section VI presents experimental results based on real time simulation and provides explanations and comments. Section VII summarizes the conclusions.

II. SYNCHROPHASOR FOR LOAD SHEDDING

A. PMUs, Synchrophasor and WAMCS

PMUs, instruments providing so-called synchronized phasor or synchrophasor measurements have been widely deployed in power systems in the last decade [27], mostly in high voltage transmission networks [18]. In the standard [28], the synchrophasor is defined as a complex number representation of either a voltage or a current, at the fundamental frequency, using a standard time reference. The synchrophasor representation A of a sinusoidal signal $a(t) = \sqrt{2}A\cos(2\pi ft + \varphi)$ is the complex value given by

$$A = A.e^{j\varphi} = A.(\cos\varphi + j\sin\varphi) \qquad \textbf{(1)}$$

Where A is the root-mean-square (rms) value of the signal a(t) , and is its instantaneous phase angle that is referred to a common reference time (UTC, Universal Coordinated Time). Both values can be measured directly by PMUs [17]. WAMCS is a central platform that may use synchrophasor measurements gathered from a wide area for the purpose of centralized monitoring and control, such as for assessing and maintaining stability [16]–[19]. The time-stamped synchrophasor data are calculated by the PMUs at high rate and with high accuracy [20]. Hence they are very effective for tracking the dynamic evolution in the power system operation, especially in critical conditions, such as the occurrence of oscillations and large disturbances [19]. Large disturbances are caused mainly by lines or generators tripping, whose connection/disconnection status monitoring can be supported by PMUs as in [10]. Therefore, synchrophasor measurements facilitate global awareness of the system. This is beneficial for the stability assessment and load shedding.

B. Role of Synchrophasor Measurements in the Proposed Load Shedding Scheme

Synchrophasor measurements have enabled new applications, including combinational load shedding using both frequency and voltage information [19]. While in traditional supervisory control and data acquisition (SCADA) systems, generally only the non-synchronized magnitude measurements of the signals are received directly from Remote Terminal Unit (RTU), which are designed for lower rate and accuracy. Furthermore, the phase angle has to be estimated via power flow calculation, which is a time consuming process. Instead, using the phase angles available directly as PMU measurements, the monitoring in power systems can be significantly improved [20], especially for centralized applications such as power flow analysis and systematic voltage stability assessment. In summary, the WAMCS system and PMUs provide the environment for implementing

UVLS and UFLS together in the same platform, thus facilitating the realization of adaptive combinational load shedding. In the proposed load shedding scheme, the phasor measurements are used in each step of load shedding procedure, as shown in Table I.

TABLE I: Phasor Measurements For Different Issues And Steps Of Load Shedding

Role	Measurements needed from PMUs	Involvement in load shedding
Frequency stability assessment	the frequency and the rate of change of frequency of each generator, and the frequency deviation of each load bus	step 1, 2, 3
Voltage stability assessment	the voltage magnitude and phase angle of each bus	step 1, 3
Power flow tracing	the voltage magnitude and phase angle of each bus	step 3

C. Voltage Stability Assessment Based on Modal Analysis

Modal analysis based on the Jacobian matrix in (2) is an efficient analytical method for global voltage stability assessment [29]–[31]: It is assumed in this paper that the Jacobian matrix is calculated by directly using the measured magnitude and phase angle values of the voltage from PMUs. In order to extract the relationship between reactive power and voltage magnitude $\Delta P = 0$ is a usual assumption to obtain the following simplified relationship as [29], [30]:

$$\Delta Q = \left[J_{QV} - J_{Q\theta} J_{P\theta}^{-1} J_{PV}\right] \Delta V = J_R \Delta V \qquad (2)$$

So, the relationship can also be expressed as

$$\Delta V = J_R^{-1} \Delta Q \qquad (3)$$

In practice, instead of calculating the J_R^{-1} directly, a decomposition method is usually applied, according to (5):

$$J_R^{-1} = E_R \xi^{-1} E_L \qquad (4)$$

So (4) can be transformed to

$$\Delta V = E_R \xi^{-1} E_L \Delta Q = \sum_l \frac{E_{R,l} E_{L,l}}{\lambda_l} \Delta Q \qquad (5)$$

where

E_R : right eigenvector matrix of J_R ;

E_R : left eigenvector matrix of J_R ;

ξ diagonal eigenvalue matrix of J_R ;

$E_{R,l}$: l th column of E_R ;

$E_{L,l}$: l th row of E_R ;

λ_l : l th eigenvalue of J_R and the corresponding mode.

The corresponding th modal voltage variation is

$$\Delta V_{ml} = \frac{\Delta Q_{ml}}{\lambda_l} \qquad (6)$$

If $\lambda_l \le 0$, the th modal voltage collapses. Correspondingly, the minimum eigenvalue $\lambda_{\min}$ stands for the mode that is the most prone to collapse, and thus it can be used as an indicator for the voltage stability of the whole system [29]. Moreover, V-Q sensitivity at bus k; can be computed [29] by

$$VQS_K = \frac{\partial V_K}{\partial Q_K} = \sum_l \frac{\mu_{kl} \cdot \eta_{lk}}{\lambda_l} \qquad (7)$$

Where μ_{kl} is the th element of $E_{R,l}$, while η_{lk} is the k th element of $E_{L,l}$. A positive value of VQS_K indicates that the relationship between the change of voltage and the change of reactive power is stable at bus K , and the voltage is more sensitive to reactive power variation as VQS_K increases. A negative value of VQS_K represents an unstable operating condition [29]. The indices for voltage stability assessment based on modal analysis are used in this paper as follows:

- $\lambda_{\min}$ is applied in the load shedding trigger determination from a global perspective; also an evaluation index for different methods comparison in the recovered steady state after load shedding;
- VQS_K is applied in the reactive power load shedding distribution. 2.4Power Flow Tracing Method for Load Shedding Distribution

Originally, power flow tracing is a method to determine the proportional usage of lines and generators by the power consumers, and then the results will act as the reference for charging in the electricity market. As a mature technology, now power flow tracing has been widely applied in the study of the power system analysis, including load shedding. This method is based on power flow results which can also be calculated using voltage magnitude and phase angle measurements supplied directly by PMUs. The so-called proportional sharing principle, both with the same computational burden. The only difference lies in the way to apportion the line loss to the side of loads or generators. The downstream-looking algorithm is applied in this paper to trace the power of each load bus received from each line and generator, and its main process is described as follows [33]. According to the principle that the inflow equals the outflow at any bus, the outflow of bus can be defined as

$$P_g = \sum_{h \in D_g} \left|P_{hg}\right| + \sum_{h \in D_G} \left|Ploss_{gh}\right| + P_{Lg} \qquad (8)$$

Where D_g is the set of buses supplied directly by bus g

$$P_{Gg,LK} = \frac{P_{Gg,} P_{LK}}{P_g} . e_g^T A_d^{-1} e_k \qquad (9)$$

where e_g and e_k represent the unit column vector where the g th or k th element equals one and the others are zeros; P_{Gg} is the active power supplied by the generator at the th bus, while P_{LK} is the total active power consumed at the th bus. Correspondingly, the contribution from the active power flow of line to the active power load of the k th bus is calculated as

$$P_{Bgh,LK} = \frac{|P_{gh}|.P_{LK}}{P_G}.e_g^T A_d^{-1} e_k \quad \textbf{(10)}$$

Where P_{gh} is the active power flow from bus g to bus h.Similarly, the reactive power flow tracing can also be defined. Therefore, the obtained tracing active and reactive powers from the generators and lines to load buses provide guidance for deciding the load shedding distribution in terms of power. All in all Where, $P_{tracing,k}, Q_{tracing,k}$: total active and reactive power at the th load bus received from the tripping generators and lines before the disturbance, calculated by means of power flow tracing approach.

III. DESCRIPTION OF THE EXISTING LOAD SHEDDING PROCESS

A. Trigger for Load Shedding

The trigger is a signal that starts the load shedding action. As the first step of conventional load shedding, trigger is always based on frequency or voltage information independently [5], [10], [34]. A local method to activate the trigger by considering both voltage and frequency jointly at each bus has been proposed in [2] and [3]. The details of each trigger used in this paper are introduced in Section IV-

B. Power Imbalance Estimation

As an important feature of adaptive load shedding method, the total power imbalance should be estimated adaptively according to different disturbances [5]. The estimation method is based on a low-order system frequency response (SFR) model [4] which is applied to estimate the active power deficit of the i th generator as shown in (14). The initial rate of change of frequency required in the calculation of (14) can be obtained from PMUs. These data are expected to be sent to control center, so that the active power imbalance ΔP_{Gi} of the i th generator can be estimated as soon as the disturbance occurs by

$$\Delta P_{Gi} = [P_{mi} - P_{ei}] = \frac{2H_i.S_i}{f_n}\frac{df_{Gi}}{dt} \quad \textbf{(11)}$$

Where, H_i : inertia constant of the th generator;

S_i : rated apparent power (MVA) of the th generator;

f_n : rated system frequency (50 Hz in this paper);

f_{Gi} : frequency of the th generator;

P_{mi} : mechanical power of the th generator;

P_{ei} : electrical power of the th generator.

Adding the individual estimated active power deficits of the generators in the power system, we can estimate the total active power imbalance ΔP :

$$\Delta P = \sum_{i=1}^{N} \Delta P_{Gi} \quad \textbf{(12)}$$

Where N is the total number of generators. Combining the two (14) and (15), together with the frequency for the equivalent inertial center as defined in [5], a new equation can be obtained as

$$\Delta P = \frac{2\sum_{i=1}^{N} H_i.S_i}{f_n}\frac{df_c}{dt} = \xi\frac{df_c}{dt} \quad \textbf{(13)}$$

where $\frac{df_c}{dt} = \frac{\sum_{i=1}^{N} H_i.S_i.\frac{df_{Gi}}{dt}}{\sum_{i=1}^{N} H_i.S_i}$, the rate of change of frequency for the equivalent inertial center; constant value.

C. Existing Methods for Load Shedding Distribution

After estimating the total power imbalance, this step focuses on determining the exact shedding amount of each load bus. Conventional load shedding distribution uses the information of $\frac{df}{dt}$ [6] or frequency change Δf [7] at each load bus, together with the initial loading condition. Considering that the large disturbance may cause the value of $\frac{df}{dt}$ of load buses to be unreliable in the process of load shedding distribution [34], Δf is usually selected as the representative frequency information used in load shedding distribution. The amount of active power load to be shed at the j th load bus, denoted as ΔP_{Lj} , is given according to [7], by

$$\Delta P_{Lj} = \frac{\Delta f_{Lj}.P_{L0,j}}{\sum_{j=1}^{M}(\Delta f_{Lj}.P_{L0,J})}.\Delta P \quad \textbf{(14)}$$

Where, Δf_{Lj} : frequency deviation at the th load bus compared to the rated frequency (50 Hz in this paper);

$P_{L0,j}$: Amount of active power load at the th bus before disturbance;

M : total number of load buses.

In this method for load shedding distribution, a load bus with heavier initial load and a larger frequency deviation ends up with a larger share of load curtailment. Besides, there is another group of methods that utilize the voltage information

in load shedding distribution. In [11], local voltage stability index called VSRI and voltage deviation are applied for small and large disturbance, respectively. As large disturbance is assumed in this paper, only voltage deviation is taken into consideration as suggested in [11]:

$$\Delta P_{Lj} = \frac{\Delta V_{Lj}}{\sum_{j=1}^{M}(\Delta V_{Lj})}.\Delta P \quad \textbf{(15)}$$

ΔV_{Lj} :voltage deviation at the th load bus compared to the voltage before the disturbance. While in [12], voltage deviation and index VQS as defined in (8), are used in allocating the total load curtailment as

$$\Delta P_{Lj} = \frac{\Delta V_{Lj} \big/ VQS_j}{\sum_{j=1}^{M}\left(\frac{\Delta V_j}{VQS_j}\right)}.\Delta P. \quad \textbf{(16)}$$

However, the reactive power is not involved in the calculation of (19).Moreover, the information used in (19) are not based on the synchrophasor measurements. Thus, there is no guarantee on the accuracy and speed for application.

IV. PROPOSED METHOD FOR LOAD SHEDDING

In the proposed adaptive combinational load shedding method, both voltage and frequency information are used in all the three main steps, as mentioned in Section I.

A. Triggering for Load Shedding

In this work, the use of global triggers is proposed. Therefore, we consider simultaneously $\lambda_{\min}$, f_c and $\frac{df_c}{dt}$ as the triggers with corresponding thresholds:

$\lambda_{\min}$: the minimum eigenvalue of the Jacobian matrix smaller than zero;

f_c : out of the normal frequency range [49.5, 50.5] Hz;

$\frac{df_c}{dt}$: the rate of change of frequency in the abnormal range of $[-1.5,-0.2]\frac{Hz}{s}$. As summarized in the IEEE UFLS standard [34], total amount of shedding load ranges from 5% to 20%, combining with (16) the values of $\frac{df_c}{dt}$ can be calculated. Therefore, depending on the fault type, any of the triggers may exceed the individual threshold thus initiating the load procedure.

B. Improved Power Imbalance Estimation

In the classic SFR model, only inertia constant of generator and frequency information are considered. However, as suggested in IEEE standard for UFLS [34], the load model with voltage and frequency dependence should also be included in the design for UFLS in order to achieve accurate active power imbalance estimation. Since the voltage variation is always much faster and larger than the change of frequency [9], only the voltage dependence of load model as in (20), is applied in the load shedding scheme in this paper:

$$P_{L,j} = P_{L0,j} \times \left(\frac{V_j}{V_{0,j}}\right)^{\alpha j} \quad Q_{L,j} = Q_{L0,j} \times \left(\frac{V_J}{V_{0,j}}\right)^{\beta} \quad \textbf{(17)}$$

$$P_L = \sum_{j=1}^{M} P_{L,j}, \quad Q_L = \sum_{j=1}^{M} Q_{L,j} \quad \textbf{(18)}$$

M : total number of load buses.

Based on this load model, the method proposed in [9] is adopted in this paper to improve active power imbalance estimation. The total active power imbalance of all the generators considering the voltage dependent load modelling, $\Delta P_{improvement}$ is defined as

$$\Delta P_{improvement} = \Delta P + \sum_{j=1}^{M} P_{L0,j} \times \left[\left(\frac{V_j}{V_{0,j}}\right)^{\alpha j} - 1\right] \quad \textbf{(19)}$$

Where ΔP is the total active power imbalance of all the generators based on the classic SFR model, neglecting the voltage dependence and frequency dependence of the load, as defined in (15). By means of the comprehensive model introduced in this section, a more accurate and rational total active power imbalance can be estimated.

$$\Delta Q_{improvement} = \frac{Q_{L0}}{P_{L0}}.\ \Delta P_{improvement}. \quad \textbf{(20)}$$

C. New Method for Load Shedding Distribution

This section focuses on a proposal to improve the load shedding distribution method, and constitutes the main contribution of this paper. Since the same total power imbalance is possible to shed at different locations of load buses, the process may lead to different new steady states after load shedding. These steady states may also not achieve system stability [15]. From this point of view, load shedding distribution is crucial for the effect of the load shedding scheme in general. Although the existing methods as mentioned in (17), (18) and (19) could be valid solutions for the distribution of load shedding, there are still two major challenges needed to be tackled:

- Reactive power is not considered in the load shedding distribution: this may lead to a deficient load shedding distribution, thus reducing the effect of load shedding;
- Voltage stability issue is not addressed jointly with reactive power: there is no guarantee of voltage stability, and the separation of voltage and reactive power may provide fallacious information to load shedding distribution, thus weakening the effect of load shedding.

Considering these two points, a new process for the load shedding distribution is proposed here. The core idea of the proposed method is to consider the active and reactive power jointly, in the determination of load shedding distribution. To this end, two indices, the load shedding distribution factor for active power (LSDFP) and load shedding distribution factor for reactive power (LSDFQ) for the load buses, are defined. LSDFP and LSDFQ can be obtained by (24), which is proportional to the total active and reactive power imbalance, respectively, as shown in (25). As seen in (24), information about frequency and active power are included in LSDFP, while voltage and reactive power information are calculated together for LSDFQ. However, in the load shedding distribution methods previously mentioned, as in (17), (18) and (19), only the LSDFP is needed. As another improvement, the initial load is replaced by the tracing power flow, to select more effective thus less load buses into shedding processing. So, in summary

$$\begin{cases} LSDFQ_j = \dfrac{VQS_j.Q_{tracing,j}}{\sum_{j=1}^{M}(VQS_j.Q_{tracing},j)} \\ LSDFP_j = \dfrac{\Delta f_{Lj}.P_{tracing,j}}{\sum_{j=1}^{M}(\Delta f_{Lj}.P_{tracing,j})} \end{cases} \quad \textbf{(21)}$$

$$\begin{cases} \Delta P_{Lj} = \Delta P_{improvement}.LSDFP_j \\ \Delta Q_{Lj} = \Delta Q_{improvement}.LSDFQ_j \end{cases} \quad \textbf{(22)}$$

Where, Δf_{Lj} : frequency deviation to the rated frequency (50 Hz in this paper) of the j th load bus; VQS_j : sensitivity of voltage variation to reactive power of the j th load bus. Afterwards, ΔP_{Lj} and ΔQ_{Lj} are determined according to (24) and (25), and then active and reactive power load shedding at each load bus can be carried out separately in theory. However, the situation is totally different in practice: load shedding is usually operated according to ΔP_{Li} which leads to the corresponding reactive power curtailment $\Delta Q'_{Lj}$. It means that the controllability of reactive power is not taken into account. In simulation, there is always an implicit assumption that, if a load is cut off, this leads to both active and reactive power curtailment, and the ratio is decided by the power factor of their initial load before disturbance as shown in (26):

$$\frac{\Delta Q'_{Lj}}{\Delta P_{Lj}} = \frac{Q_{L0,j}}{P_{L0,J}}. \quad \textbf{(23)}$$

Therefore, there is a mismatch between ΔQ_{Lj} , as determined by reactive power load shedding, and $\Delta Q'_{Lj}$, caused by the curtailment action only according to the active power. This difference, though, can be compensated by the reactive power compensating devices such as the static compensator (STATCOM), static VAR compensator (SVC), switching capacitor banks and so on. Moreover, the calculated amount of reactive power to be shed in the proposed method can be distributed as an additional reference signal to the local reactive power compensation sources like switching capacitor banks. It can also be regarded as a kind of coordinated reactive power compensation from the point of view of the overall system during the load shedding.

D. New Indices for Evaluating the Effect of Load Shedding on Load ability

Due to the load model in (20) and the improved power imbalance estimation in (22) applied in this paper, three new indices are selected as metric for evaluating the effect of load shedding. The indices are defined as follows:

$P_{loss,after}$: the total active power loss of the whole network in the recovered steady state after load shedding;

$P_{L,after}$: the total active power load in the recovered steady state after load shedding;

$Q_{L,after}$: the total reactive power load in the recovered steady state after load shedding .

Notice that $P_{L,after}$ and $Q_{L,after}$, do not simply equal the initial total load minus the total power imbalance. Since the load modelling in the form of voltage dependence is applied in this paper, $P_{L,after}$ in (27) and $Q_{L,after}$ in (28) are determined as the amount of load shedding and voltage of each load bus together in the recovered steady state. Essentially, $P_{L,after}$ and $Q_{L,after}$ are closely dependent to the allocation of load shedding:

$$P_{L,after} = \sum_{j=1}^{M}\left[(P_{L0,j} - \Delta P_{Lj}) \times \left(\frac{V_{j,after}}{V_{0,j,after}}\right)^{\alpha j}\right] \neq P_{L0} - \Delta P_{improvement} \quad \textbf{(24)}$$

$$Q_{L,after} = \sum_{j=1}^{M}\left[(Q_{L0,j} - \Delta Q_{Lj}) \times \left(\frac{V_{j,after}}{V_{0,j,after}}\right)^{\beta j}\right] \neq Q_{L0} - \Delta Q_{improvement} \quad \textbf{(25)}$$

where:

$V_{0,j,after}$: the initial voltage magnitude of the j th load bus after load shedding;

$V_{j,after}$: voltage magnitude of the j th load bus in the steady state after load shedding.

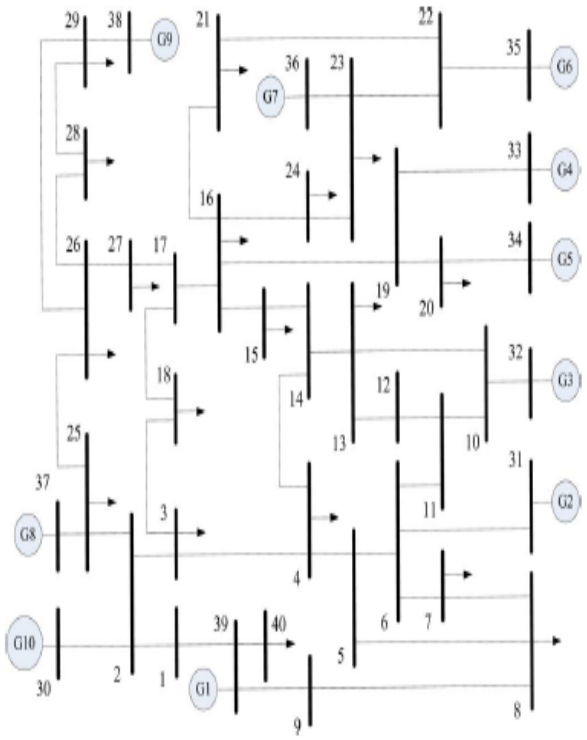

Fig. 1. Topology of modified IEEE 39-Bus system.

TABLE II: The Description About Modified Ieee 39-Bus System

Number of buses	Number of generators	Number of loads	Number of lines	Number of transformers
40	10	18	35	12

V. TEST SYSTEM AND TESTING PLATFORM

A. Test Case

As a typical transmission network with multiple generators, IEEE 39-Bus test system (New England network) [35] is selected as an example in this paper. Seen from Fig. 1, a small modification is to divide bus 39 into bus 39 with a load and bus 40 located with a generator, which are connected by a transmission line with low impedance, while the small load in bus 31 is neglected. A short summary of the network characteristics is given in Table II. Two assumptions are made for the PMUs:

- full network observability is ensured by the PMUs located in this system;
- PMUs are able to provide the complete information about each bus involved in the load shedding process.

B. Modelling in RTDS Simulation

The power network in Fig. 1 is simulated in Real Time Digital Simulator (RTDS) [36]. RTDS is a powerful platform which performs real time simulation of power systems by a combination of customized software and hardware, with a fixed time step of 50 μs (or less for specific schemes). The reason for this choice lies in that RTDS simulates the full dynamic behaviour, essential for the load shedding research. In addition, this implementation is ready for the extension of our proposed load shedding method to on-line operation, for the real-time control research and test with hardware in the loop techniques. In the RTDS simulation, the rated frequency of the system is 50 Hz, while the reference voltage and the reference power are chosen by 345 kV and 100MVA, respectively. The synchronous machines are used for generator modelling, with the IEEE Type 1 Excitation System and IEEE Type 1 Governor/Turbine control models.

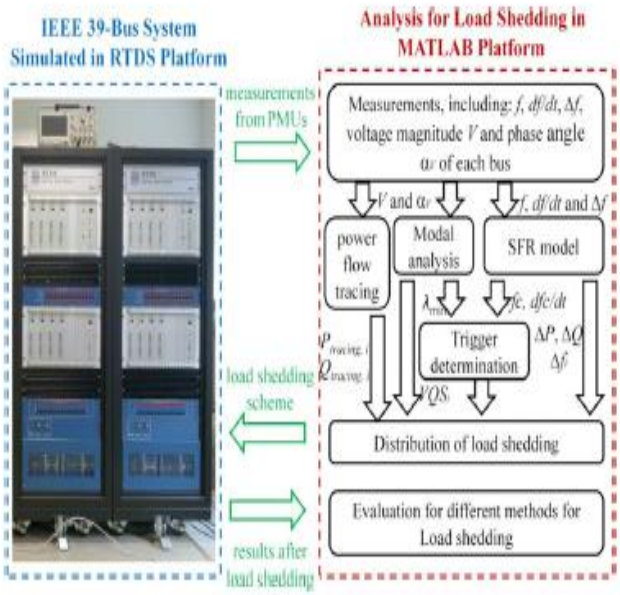

Fig. 2. Configuration of the testing platform.

The ratios of the step-up transformers are chosen by 13.8/345 kV and its wire style is lagging $Y-\Delta$. The transmission lines are modelled with ideal RLC components, and realistic transmission line models are used for connecting the subsystems modelled in three different racks. For each load bus, as mentioned in (20), the exponential coefficient load model (only considering voltage dependence) is adopted, whose active and reactive power varies dynamically as voltage changes in runtime. According to the standard [28], the reporting rate of PMUs 25 Hz is an available option and is selected in the subsequent simulation, which means synchrophasor measurements are collected from PMUs every 40 ms and all the analysis are required to complete within such time interval.

C. Testing Platform

As shown in Fig. 2, the testing platform constitutes of two aspects: power system simulation in RTDS and analysis in MATLAB [37]. The synchrophasor measurements used for load shedding are collected from the PMU components of RTDS. First, a collapse process without any load shedding

action is recorded. The saved data is imported into MATLAB for the off-line computation, such as f_c and $\frac{df_c}{dt}$ for the equivalent inertial center, power imbalance estimation, tracing power flow $P_{tracing,i}$ and $Q_{tracing,i}$, indices $\lambda_{\min}$ and VSQ_i about the voltage stability, and the amount of load curtailment distributed to each individual load bus. According to the results provided by MATLAB, the load shedding scheme can be drawn up and implemented back into the RTDS simulation for test, hence the corresponding data is recorded and sent back to MATLAB again, to check the effect of the load shedding.

D. Time Burden in the Centralized Application

For the centralized application as proposed in this paper, there are two main challenges related to time: communication delay by transmitting PMU measurements to the control center and calculation time for central analysis based on the Jacobian matrix. For the latter, as for computing the minimum Eigen value of Q-V Jacobian and power flow tracing, no iteration process is needed, since the magnitude and phase angle of voltage are

TABLE III: Time Burden Caused By Different Issues

Issues	Commun-ication (time delay)	Analysis			
		Modal analysis	Power flow tracing	Disturbance estimation (total load shedding)	Load shedding distribution
Time burden	Less than 100 ms [10][39]	5 ms	8 ms	< 2 ms	< 2 ms

TABLE IV: Classification of Methods for Load Shedding

Method No.	Factors in load shedding distribution	
	LSDFP	LSDFQ
M1	Δf_{Li} and initial active power $P_{L0,i}$	equal to LSDFP
M2	ΔV_{Li}	equal to LSDFP
M3	ΔV_{Li} and $1/VQS_i$	equal to LSDFP
M4	$P_{tracing,i}$ and Δf_{Li}	$Q_{tracing,i}$ and VQS_i

M1: corresponds to existing distribution method as defined in (17); M2: corresponds to existing distribution method as defined in (18); M3: corresponds to existing distribution method as defined in (19); M4: corresponds to the distribution method as mainly defined in (24) and (25), proposed in this paper. directly provided by PMUs, instead of being calculated conventionally by iterative power flow or state estimation. Therefore, the computing time is very low. As for the communication delay of PMUs, this can vary from milliseconds to seconds [28]. according to the survey to the TSOs and research facilities in Nordic Region [38]. Therefore, a load shedding procedure that can react within such time range, which may make the time issues not critical. For addressing the time issues more clearly, the expected time burden of the main operations are listed in Table III. For the analysis part, all the results about computation time are obtained with MATLAB 2010b operating in the PC environment of Intel Core 2 Quad CPU Q8400 at 2.66 GHz.

VI. TESTING RESULTS AND DISCUSSION

A. Classification of Load Shedding Methods

According to the distribution of load shedding, four load shedding methods are summarized here and denoted as M1, M2, M3 and M4 in Table IV. The common point is that they have the same first and second step in the load shedding process. All the information needed in each load shedding distribution method is also included in Table IV. The subsequent tests are carried out for comparison purpose.

B. System Collapse without Load Shedding

The simultaneous tripping of generator 3 and transmission line (5, 6) is assumed in this test scenario. The generator and transmission line play a significant role in the system, based on the large respective generation and transmission capacity in

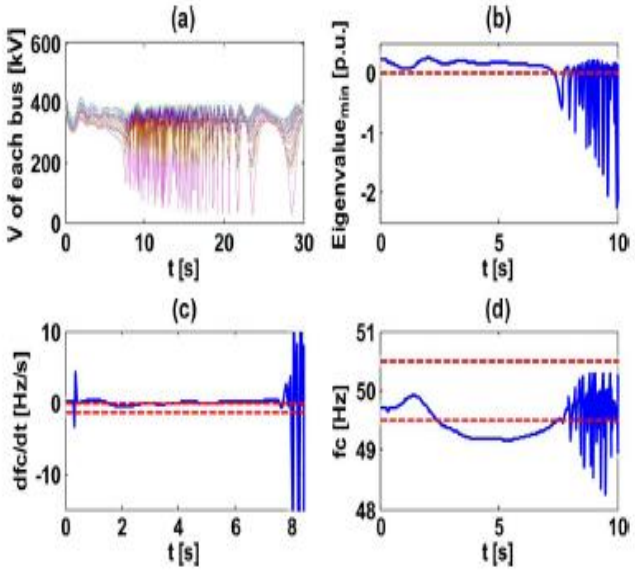

Fig. 3. Observation for the system collapse process without load shedding.

Steady condition before the disturbance occurs. Therefore, the tripping of them leads to an active power deficit accompanied by a reactive power deficit in the test scenario. The evolution of the test condition is recorded for 30 s. In simulation the disturbance occurs at 0.3 s. The voltage magnitude of each bus immediately undergoes a slight fluctuation, sustained for approximately 7 s, then falls into severe oscillation, as shown in part (a) of Fig. 3. Part (b) to part (d) of Fig. 3 are zoomed in to

concentrate on the transient process after disturbance, and the red dashed lines denote the threshold for each trigger as mentioned in Section IV-A. According to the global voltage stability assessment with the minimum eigenvalue $\lambda_{\min}$ as discussed in Section II-C, voltage collapse is determined at about 7.4 s as shown in part (b). Seen from part (c), the rate of change of the frequency $\frac{df_c}{dt}$ immediately presents a sudden glitch at 0.04 s after disturbance. This transient highly depends on the dynamic response of generators with excitation and governor control, loads and other dynamic devices as described in [5], while part (d) indicates the value of frequency changes slowly and moves out of normal frequency range at 2.44 s, hence starting to frequency oscillation. Therefore, this disturbance causes voltage and frequency instability simultaneously, but the trigger is firstly activated by the change of $\frac{df_c}{dt}$. Since no load shedding action is taken, eventually all the generators are out of step and the system falls into serious oscillation.

D. LSDFP and LSDFQ in Load Shedding Methods

As defined in Table IV, LSDFP of methods M1, M2 M3 and M4 together with LSDFQ of method M4 are shown in Fig. 4 shows that LSDFP of M1, M2 and M3 yield different effects even for a same bus, while the total amount of load curtailment is shared uniformly by each load bus. For M4, the LSDFP and LSDFQ of each bus are different, which demonstrates active power and reactive power have different properties for sharing the respective total load curtailment. If we ignore the LSDFQ or just simply assume that they are identical, this may lead to an inaccurate load shedding distribution, thus bringing to a less effective load shedding scheme, according to the following test results. Also notice that not all the load buses are involved into load shedding in M4, which instead concentrates the burden on few load buses in vicinity of the tripping generator

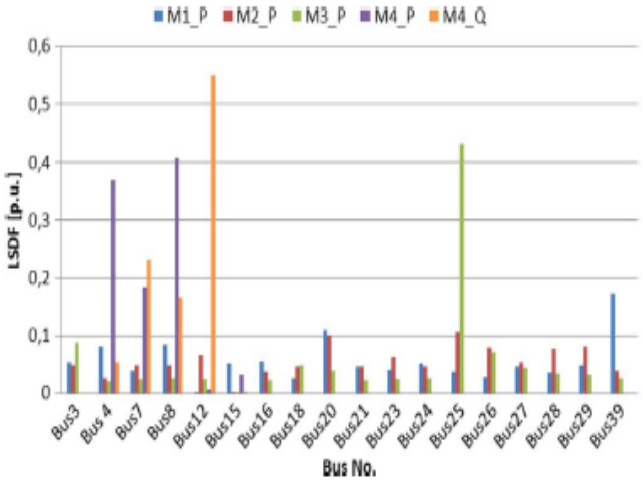

Fig. 4. Load shedding distribution factor of each method.

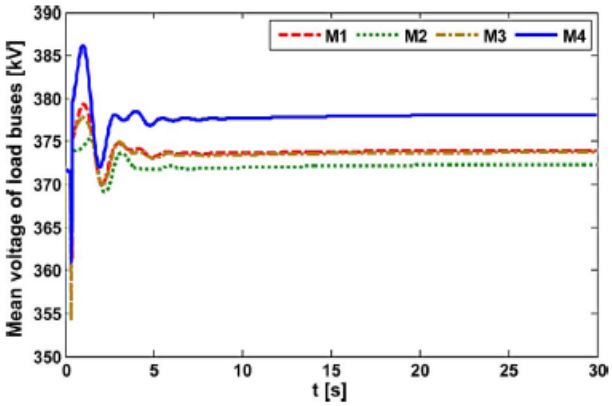

Fig. 5. Mean voltage of all the buses in the load shedding process.

And transmission line, for instance bus 4, 7, 8 and 12. The critical difference lies in the fact that power flow tracing method is only applied inM4. Therefore, this result reveals the main advantage of power flow tracing when applied in load shedding distribution: it can contribute to focus on some load buses to narrow the sharing scale among the load buses, instead of dividing total power imbalance uniformly to each load bus, according to the information such as the initial load before disturbance.

E. Comparison of Transient Behaviour of Different Load Shedding Methods

Since the same disturbance is applied to test all load shedding methods, and as all the methods obtain $\Delta P_{improvement}$ as defined in (22), the total active power imbalance is identical for all methods. As observed from the results, the system can always escape from collapse, and stay at different new steady states depending on the chosen methods for load shedding distribution. The whole process of load shedding with different methods is reported from Figs. 5–8. As shown in Fig. 5, the mean voltage of all the buses of the four methods have similar behaviour presenting a fast and large drop when disturbance occurs and settling at a new value after a short oscillation thanks to load shedding actions.

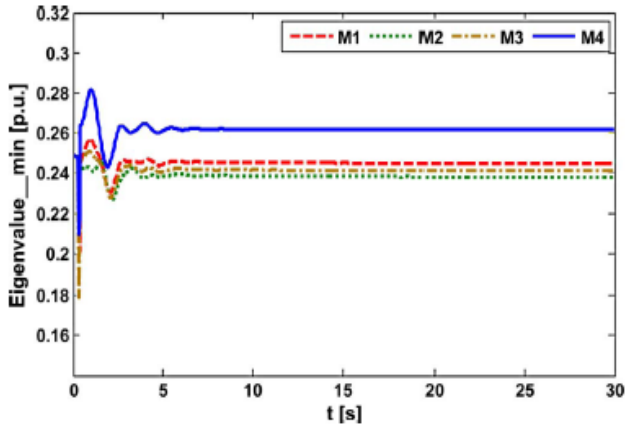

Fig. 6. Minimum eigenvalue of each method in the load shedding process.

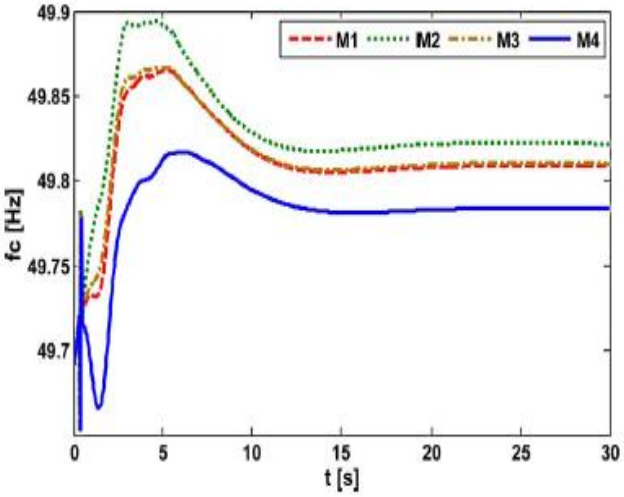

Fig. 7. f_c **of each method in the load shedding process.**

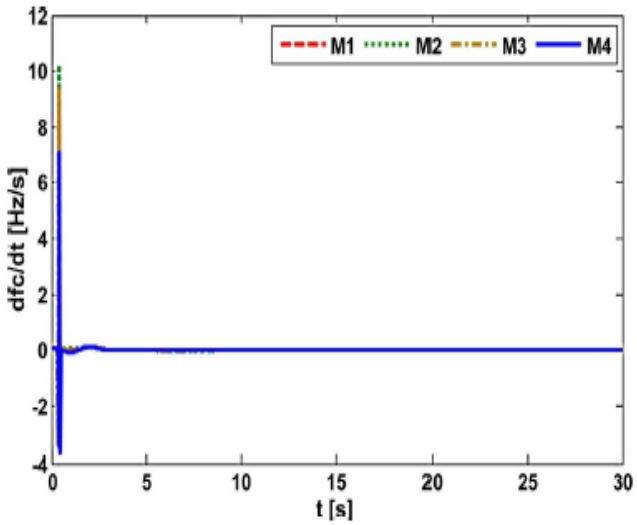

Fig. 8. $\frac{df_c}{dt}$ **of each method in the load shedding process.**

This result indicates that all the methods are effective to prevent system from collapsing, and are able to move it into a new steady state after load shedding. Figs. 6–8 report the comparisons of $\lambda_{\min}$, f_c , and $\frac{df_c}{dt}$ for all the four methods: during the process from steady state before disturbance to the system recovery. In Fig. 6, $\lambda_{\min}$ of M4 is always higher than the others in positive ranges, even during the short oscillation, which means thatM4 keeps the system voltage more stable all the time. Fig. 7 is about the recovering of the frequency for the equivalent inertial center f_c f . It shows that the amplitude of the oscillation of M4 is the smallest. Seen from Fig. 8, the difference of $\frac{df_c}{dt}$ is minimal among the methods.

TABLE V: Comparison among Load Shedding Methods during the Transient Process,

Conditions	Evaluation Indices			
	maximum deviation of f_c (Hz)	*maximum deviation of* V_{mean} (kV)	*Oscillation duration of* f_c (s)	*Oscillation duration of* V_{mean} (s)
M1	0.1551	12.55	14.18	8.94
M2	0.1415	24.35	14.30	10.18
M3	0.1495	15.69	13.54	8.94
M4	0.1303	17.22	15.34	8.82

Which means this index is weakly impacted by the load shedding distribution method. To quantify the results during the transient process, the maximum deviation of and the maximum deviation of f_c mean voltage V_{mean} of all load buses during the transient process, and the time for the f_c and V_{mean} to re-settle to a new steady-state value are also used as significant indices. Referring to the definitions for maximum deviation and oscillation duration for rotor speed in [40], we applied them to the analysis of the transient process of voltage and frequency oscillation in this paper. The oscillation duration t_{osc} is defined as

$$t_{osc} = t_{new\_steady} - t_f \qquad \textbf{(26)}$$

Where is the time when the fault occurs, which is 0.3 s in our test; while is the time when the system reaches a new steady state after load shedding. Normally, is determined by the change of , which is the value of or at time point , once it is sufficient small in a continuous period of time, as defined in the following:

$$t_{new\_steady} = \min\{t : |z(t+n.\Delta t) - z(t)| \le \mu; \quad n = 1,2,...,10\} \qquad \textbf{(27)}$$

Where Δt is set as 0.04 s corresponding to the reporting rate of PMUs. The maximum deviation of f_c and V_{mean} are defined as

$$\Delta_{z\max} = \max\left\{\left|z(t) - z_{new\_steady}(t)\right|\right\} \qquad \textbf{(28)}$$

where $z_{new\_steady}(t)$ is the value of $z(t)$ at the time point t_{new_steady}. The test results can be found in Table V. These indicate that the maximum deviation of f_c caused by M4 is the smallest, but the corresponding oscillation duration is the longest. This is because of the best load ability of M4 as shown in the next subsection, which is not beneficial to damping the oscillation of frequency. While M4 does not experience the largest voltage oscillation in the transient

process, voltage recovers fastest to the new steady state with the highest magnitude. Hence, the voltage stability issue is well addressed by considering the reactive power and voltage as a pair individually in the process of load shedding distribution.

TABLE VI: Comparison among Load Shedding Methods In Frequency And Voltage

Conditions	Evaluation Indices				
	f_c (Hz)	λ_{min} (p.u.)	V_{max} (kV)	V_{mean} (kV)	V_{min} (kV)
Before disturbance	49.71	0.2482	383.66	371.18	356.10
M1	49.81	0.2434	387.46	373.64	359.49
M2	49.82	0.2443	386.94	374.75	361.19
M3	49.80	0.2489	387.93	374.84	360.76
M4	49.78	0.2607	386.40	377.42	366.15

F. Comparison of Recovered Steady State in Aspect of Voltage and Frequency

To compare the effective of different load shedding methods, some evaluation indices are needed to distinguish the characteristics of the new steady state after disturbance and the corresponding action of load curtailment. Including the steady states before disturbance and after load shedding with four methods, five aspects are considered. First, the frequency for the equivalent inertial centres f_c of the system and the indices of voltages of all the load buses are compared as shown in Table VI. There is only a minor difference in f_c among the methods, which indicates that the frequency of the system in new steady state is mainly determined by the total amount of load shedding, considering that active power imbalance is identical for all the methods. In terms of higher $\lambda_{\min}$, M4 is able to bring the system into a new steady state with more stable voltage, for the same total load to be shed. Moreover, it indicates that the best voltage profile in M4 is kept in the new steady state, regardless of the mean and minimum voltage of all the load buses.

TABLE VII: Comparison Among Load Shedding Methods In Power

Conditions	Evaluation Indices		
	$P_{loss,after}$ (MW)	$P_{L,after}$ (MW)	$Q_{L,after}$ (MVar)
M1	47.90	5821	1246
M2	53.11	5826	1178
M3	56.69	5855	1284
M4	40.05	5911	1324

G. Comparison of Recovered Steady State In Aspect Of Load Ability

In Table VII, three new indices as defined in Section IV-C are used for evaluating the test results. As it can be seen from Table VII, M4 achieves the least total active power loss of network in the new steady state, although the new steady state is only a temporary period which is usually not sustained for a long time. Interesting comparison information are provided by $P_{L,after}$ and $Q_{L,after}$, which are not included in previous research work. In this comparison, the effect of M4 is the best since both active and reactive power loading

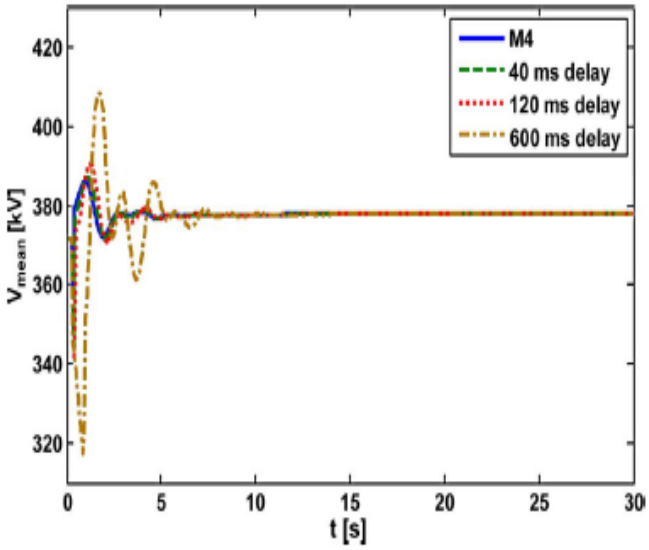

Fig. 9 V_{mean}. of method M4 with different time delays in the load shedding process.

is kept at a higher level than the others. The larger values of $P_{L,after}$ and $Q_{L,after}$ indicate the load ability in recovery condition is better after shedding identical total amount of load. The reason can be understood from two aspects: • in all the four methods compared in our paper, total amount of load shedding is identical owing to the same disturbance and same method for total active power imbalance estimation. Therefore, the total load before load shedding and total load curtailment of all the methods are identical, but the total power loading after load shedding is different depending on the load shedding distribution methods. The critical reason lies in the load model of voltage dependence [9] applied in the analysis and simulation in this work, more realistic for real power system and also suggested by the IEEE standard [34]. This decides that larger voltage magnitude leading to larger power consumption, thus the better load ability; Total load after load shedding closely depends on the voltage profiles. The better voltage profiles are achieved by taking into consideration the index VQS together with reactive power in the step that yields the distribution of load shedding. Therefore, M4 ensures the best load ability after load shedding, thanks to the better voltage profiles at individual load buses. This is achieved by means of the load shedding distribution that integrates reactive power Compensation. In summary, the proposed method M4 exhibits the best

performance in relation to steady state after load shedding from the point of view of each proposed index.

H. Impact of Time Delay Caused by Communication on Load Shedding Results

In Table III, the time delay in synchrophasor transmission is the biggest challenge for load shedding. To better investigate this aspect, we have run a sensitivity test to check its impact, setting different values of time delay in the RTDS simulation. As shown in Figs. 9 and 10, as time delay increases, the maximum deviation of f_c and V_{mean} during the oscillation becomes larger. For this test case, the limit of impact from the time delay is between 2 s and 4 s, beyond which the load shedding procedure may fail.

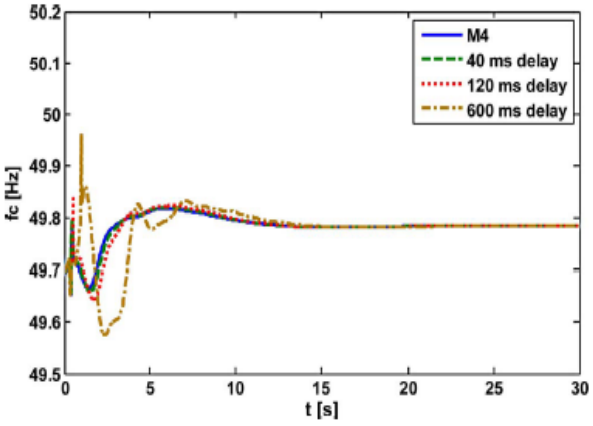

Fig. 10. of method M4 with different time delays in the load shedding Process.

TABLE VIII: Comparison Among Load Shedding Methods In Frequency And Voltage—In Condition Of Two Generators Tripping

Conditions	Evaluation Indices				
	f_c (Hz)	λ_{min} (p.u.)	V_{max} (kV)	V_{mean} (kV)	V_{min} (kV)
Before disturbance	49.81	0.2563	395.69	373.96	365.47
M1	50.00	0.3340	391.01	385.64	370.96
M2	49.96	0.3204	395.81	384.62	365.13
M3	49.85	0.2866	384.98	373.89	357.71
M4	49.93	0.3359	391.31	384.62	376.37

TABLE IX: Comparison Among Load Shedding Methods In Power—In Conditionof Two Generators Tripping

Condition	Evaluation Indices		
	$P_{loss,after}$ (MW)	$P_{L,after}$ (MW)	$Q_{L,after}$ (MVar)
M1	31.02	4927	1075
M2	41.97	5038	1098
M3	48.27	5036	1128
M4	30.41	5076	1169

I. Test Results in Condition of Simultaneous Tripping of Two Generators

To show the applicability of the proposed methods, another test scenario is studied. In this scenario, the disturbance caused by tripping of generator 5 and generator 6 simultaneously is assumed. The capacities of some generators are adjusted to allow for the system collapse in this fault condition. Similarly to the previous test results, all the load shedding methods can maintain the stability of the system after disturbance and bring the system into a new steady state. In addition, similar conclusions can be obtained from Tables VIII and IX, that the M4 is still the most effective method at strengthening the new steady state after executing the same total amount of active power curtailment.

VII. CONCLUSION

To overcome the disadvantages of the existing adaptive combinational load shedding methods, a load shedding scheme based on a new load shedding distribution method, using combined frequency and voltage stability assessment, is proposed in this work. The synchrophasor measurements are used throughout the proposed load shedding process. As an innovation of this paper, reactive power is used directly into the reactive power load shedding distribution together with active power load shedding distribution, to address the voltage stability issue directly and more effectively in the load shedding process. Also, modal analysis is chosen to address the voltage stability issue more accurately, via a sophisticated and global algorithm, which particularly benefits from phase angle measurements of the PMUs. Moreover, the power flow tracing algorithm is applied in the load shedding distribution, to select the more effective load buses and thus reducing the number of load buses for sharing the total power imbalance. The test results indicate that the improvements on load shedding distribution of load shedding method can enhance the new steady state of power systems in view of frequency stability, voltage stability and load ability, also with a good transient behaviour, when encountering the large disturbances. Thus, for the load Shedding in practical application, there is a new choice to protect the system safely and efficiently.

VIII. REFERENCES

[1] P. Kundur et al., IEEE/CIGRE Joint Task Force on Stability Terms and Definitions, "Definition and classification of power system stability ," IEEE Trans. Power Systems, vol. 19, no. 3, pp. 1387–1401, Aug. 2004.

[2] A. P. Ghaleh, M. Sanaye-Pasand, and A. Saffarian, "Power system stability enhancement using a new combinational load-shedding algorithm," IET Gen., Transm., Distrib., vol. 5, no. 5, pp. 551–560, May 2011.

[3] A. Saffarian and M. Sanaye-Pasand, "Enhancement of power system stability using adaptive combinational load shedding methods," IEEE Trans. Power Syst., vol. 26, no. 3, pp. 1010–1020, Aug. 2011.

[4] P. M. Anderson and M. Mirheydar, "An adaptive method for setting under frequency load shedding relays," IEEE Trans. Power Syst., vol. 7, no. 2, pp. 647–655, May 1992.

[5] V. V. Terzija, "Adaptive underfrequency load shedding based on the magnitude of the disturbance estimation," IEEE Trans. Power Syst., vol. 21, no. 3, pp. 1260–1266, Aug. 2006.
[6] A. V. Kulkarni, W. Gao, and J. Ning, "Study of power system load shedding scheme based on dynamic simulation," in Proc. 2010 IEEE PES Transmission and Distribution Conf. Expo., Apr. 2010,pp. 1–7.
[7] Z. Zhong, "Power systems frequency dynamic monitoring system design and applications," PhD. dissertation, Dept. Elect. Comput. Eng., Virginia Polytechnic Institute and State Univ., Blacksburg, VA, USA, Jul. 2005.
[8] U. Rudez and R. Mihalic, "Monitoring the first frequency derivative to improve adaptive under frequency load-shedding schemes," IEEE Trans. Power Syst., vol. 26, no. 2, pp. 839–846, May 2011.

Author's Profile:

Mr.A.Syed Saheb Vali was born in Andhra Pradesh, India in 1992. He received the B.Tech (Electrical and Electronics Engineering) degree from JNTU Anantapuram, India in 2013 and the M.Tech (Electrical Power Engineering) Pursuing from JNTU Anantapuram, in 2016 (Nove) he joined the Dept. Electrical and Electronics Engineering, Sreenivasa institute of Technology and Management studies as a PG-Student,
Email: sahebvali123@gmail.com.

Mr. M. Apsar Basha obtained his B. Tech degree in Electrical and Electronics Engineering from JNTU Anantapuram, India in 2010. He obtained his M. Tech degree in Power Systems, from JNT University, Anantapuram. India in 2012. Currently, he is working as Assistant Professor, Sreenivasa institute of Technology and Management studies , and he had 4 years experience. Chittoor A.P.Email:Apsar.huzaipha@gmail.com

A. Kanaka Krishna Goud student, M. Tech in Power Electronics from Sreenivasa Institute of Technology and Management Studies, Chittoor-District, Andhrapradesh, India. Graduated in B.Tech EEE in the year 2013 from Priyadharshini Institute of Technology, Ramachandrapuram, Tirupathi, Chittoor, Andhra pradesh. Research interest in Power Electronics and Drives.

Mr. Y.Radhaiah was born in Andhra Pradesh, India in 1992. He received the B.Tech (Electrical and Electronics Engineering) degree from JNTU University, India in 2013 and the M.Tech (Electrical Power Systems) from same University. In 2015 (Nove) he joined the Dept. Electrical and Electronics Engineering, Sri Venkateswara College of Engineering and Technology (AUTONOMUS)l, as a PG-Student,
Email:radhaiaheee@gmail.com.